Proceedings of the 21st ICSMGE, Vienna, Austria, 14 – 19 June 2026. Pistrol, Adam & Schweiger (eds.)
Published by: ÖGG, Austrian Society for Geomechanics, Salzburg, Austria, ISBN 978-3-9503898-4-5
https://doi.org/10.53243/ICSMGE2026-2260

Simulation of scour around wind turbine monopiles using 1D and 3D approaches

Anis Kheffache, Bruno Stuyts
UGent Geotechnical Institute, Ghent University, Belgium, anis.kheffache@ugent.be

ABSTRACT: Scour is one of the most significant and prominent hazards that can affect fixed offshore wind turbines. Scour leads to the reduction of offshore wind turbines lifetime and stability, as a consequence of loss of strength and stiffness. In terms of modeling, 1D beam-column models are generally used for the routine design of offshore wind turbines, mainly due to the simplicity associated with such approaches. The soil response is captured using non-linear spring coefficients (such as the PISA ones), and discretized along the foundation depth, which generally consists of monopiles. Although computationally heavier, 3D finite element approaches are better suited for capturing the complex soil-foundation interactions, given that a well-calibrated soil constitutive model is employed. In this work, the effect of scour is investigated on a monitored offshore wind turbine using 1D and 3D approaches. A 3D finite element model in which the soil is modeled using advanced hypoplastic sand and clay models is first validated then used. The monopile is subjected to lateral loading in both models, then the monopile's response is investigated, mainly in terms of bending moments. Conclusions are drawn and recommendations are formulated.

KEYWORDS: Offshore wind, Monopile, Finite Element, Scour, Stiffness.

1 INTRODUCTION

As the need for cleaner energy is echoed globally around the world, offshore wind is expected to play a major role in ensuring a safe energy transition. As most countries are aiming for the decarbonization of their economy, the announcement of new wind farm zones is becoming more frequent. The European goal is to collectively reach 60 and 300 GW of installed wind capacity by 2030 and 2050 respectively.

Monopiles are the preferred support structures for offshore wind turbines, mainly due to their technical and economic suitability (Kallehave et al., 2015), as the supply chain from the manufacturing to the installation is robust and well established. The monopile is also expected to still be the preferred type of foundation for most of the future wind farms, even in deeper waters, as long as technical feasibility permits.

Offshore wind turbines are dynamic structures for which the natural frequency f_0 should be designed in a narrow range, surrounded by forcing frequencies. Any phenomena leading to the change of their frequency should be well captured by the design methodology used to design such structures.

Following previous papers that focused on the monopile-soil interaction (Kheffache et al., 2024), this paper will focus on the investigation of scour effects on offshore wind turbines. Two numerical approaches are used, the first consists of a well-calibrated 3D FEM model, which employs advanced constitutive models for the modeling of soil. The second approach consists of a 1D beam-column model in which the soil response is captured using non-linear springs. The 3D FEM model is first thoroughly validated using centrifuge tests from the literature. Conclusions on the effect of scour and on the validity of 1D methods for scour analyses are drawn and recommendations are formulated.

2 SCOUR AROUND OFFSHORE WIND TURBINES

Waterflow over the seabed may be obstructed by the monopile structure, resulting in complex water flow around it which can lead to the erosion of sediments, which is referred to as scour (Sumer and Fredsøe, 2002). Two types of scour are generally referenced in the literature, global and local scour (Deltares, 2023). Global scour consists of a global lowering of the seabed level (often independent of the structure), while local scour consists of the creation of a pit around the foundation, for which the depth is referred to as scour depth.

Under wind thrust, offshore wind turbines are subjected to lateral loading, which is transmitted from the rotor down to the monopile, which in turn transfers the loads to the surrounding soil. The removal of soil around the monopile through scouring challenges the safe operation of OWTs. As an example, the Robin Rigg offshore wind farm, located in the UK is a well known case study across the offshore wind industry. As a result of global scouring, which was noticed through the monitoring of their natural frequency (drop in the first mode frequency f_0), two wind turbines were prematurely decommissioned, and remedial scour protection systems were installed at several other locations.

To date, 1D beam-column models are still the most used design methodology for offshore wind turbines, especially due to the low numerical cost associated with them. The wind turbine (monopile, transition piece and tower) is modeled using beam elements, while the soil response is captured using non-linear spring elements.

Offshore piles, especially in the Oil and Gas industry, have been designed using methods that were derived on the basis of load tests on relatively slender piles which is translated by high slenderness L/D ratios. Offshore wind turbine foundations are much less slender, as the L/D ratios generally vary between 2 and 10. The applicability of the previous methodologies is thus highly questionable. The recently completed PISA project (Burd et al., 2020; Byrne et al., 2020) proposed new sets of soil reaction curves for laterally loaded wind turbine monopiles. It was based on both advanced numerical analyses and high-quality field experiments on piles, with an L/D ratio of 2 to 6, which is comparable to that of monopiles.

3D Finite Element Method (FEM) approaches are computationally more demanding than the 1D methods, and their performance depends heavily on the model's refinement and that of the adopted constitutive laws (especially for the soil), however, they can represent the full distribution of stresses and strains in both pile and soil.

The following sections will focus on the simulation of scour around a monitored wind turbine monopile located in the Belgian North Sea, using both 1D beam column (PISA rule-based) and 3D FEM approaches.

3 NUMERICAL MODELING

3.1 *Validation of a 3D FEM model*

The 3D FEM model was validated using centrifuge tests performed by (Qi et al., 2016) on a scale pile of 11 mm and a 140 mm of diameter and length respectively. The testing scale was of 1:250, which brings the prototype diameter and length respectively to 2.75 and 35 m. The pile's bending stiffness *EI*

was of 88.1 GNm^2. The pile was embedded in the UWA silica sand, for which the index properties are well documented and won't be repeated here for brevity (Bienen et al., 2021; Spyridis and Lopez-Querol, 2024). Several tests were performed with various load eccentricities, pile embedment depths, scour types and depths. The scour depth is referred to as s and is normalized by the pile prototype diameter D. Only the cases mentioned in the following table are used for the validation.

Table 1.Conditions of the performed tests

Load eccentricity, m	Pile embedment, m	Scour depth, m
5.5	31.25	0
10.5	26.25	5
13	23.75	7.5

It should be mentioned that the scour slope was of 30° for all the cases where soil scour was considered. The load eccentricity is calculated as the distance between the load application point and the top of the soil layer (after scour). The modeling is done in ABAQUS, where an elastic model was assigned to the prototype pile, while the soil was modeled using the hypoplastic sand model (von Wolffersdorff, 1996), for which the parameters have been previously calibrated for the UWA silica sand model.

3.1.1 *No scour case*

The model is first validated using an unscoured soil profile. The pile is progressively laterally loaded with an eccentricity of 5.5 m. The load-displacement curve at the point of load application is shown in Figure 1 corresponding to an s/D of 0. The bending moments are shown in Figure 2 for different load intensities. An overall pretty good fit can be observed between both the simulated and test-monitored load-displacement and bending moment curves. The lateral *p-y* reaction curves are extracted from the numerical model using two methods: the first consists on integrating the stresses on the soil elements immediately surrounding the pile and computing the lateral forces, which are summed on every segment to build the numerical *p-y* curves, the second method consists of extracting the contact forces from every node and summing them on each segment. Both methods yielded in similar results. Figure 3 shows both the numerical and test-based *p-y* curves at different normalized depths z/D. While a small mismatch is noticed between simulated and calculated (test) *p-y* curves at shallow levels (z/D of 1 and 2), the mismatch seems lower at deeper layers (z/D of 3 and 4).

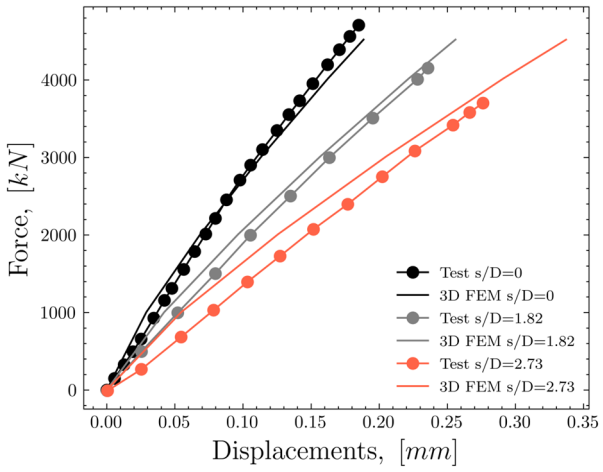

Figure 1. Force displacement curves for s/D of 0, 1.82 and 2.73

3.1.2 *Normalized scour depths s/D of 1.82 and 2.73*

In these cases, the soil was subjected to normalized scour depths of 1.82 and 2.73, then the pile was subjected to lateral loading. The corresponding load-displacement curves for both s/D values are also shown in Figure 1. It can be seen that an increase of s/D, which is essentially an increase in scour depth, leads to a decrease in the lateral stiffness and capacity of the pile. The numerical model also seems to adequately capture the load-displacement curves when compared to the test-monitored ones for both s/D values. The bending moments corresponding to a lateral load of 3 MN are shown in Figure 4 for s/D values of 0, 1.82 and 2.73. it can be seen from both numerical and test results that an increase in s/D leads to an increase of the maximum bending moment value (under the same lateral load), and a decrease in the depth of application of this point. It can be seen from the same figure that the numerical model is able to capture the monitored bending moments for all the s/D values satisfactorily. It can also be seen from Figure 5 that a good agreement is achieved between the simulated and calculated *p-y* curves for s/D of 1.82 and 2.73.

After the series of simulations presented above, it can be considered that the numerical model is validated and can be used to simulate scour around a pile. The importance of simulating the unloading (decrease of stress after scour) and the assignment of initial stresses that correspond to a scoured soil, in contrast of just modeling a removed soil volume is of importance. The proper modeling of the unloading is, of course related to the constitutive model's ability to replicate the soil's stiffness dependency on effective stresses, and void ratio.

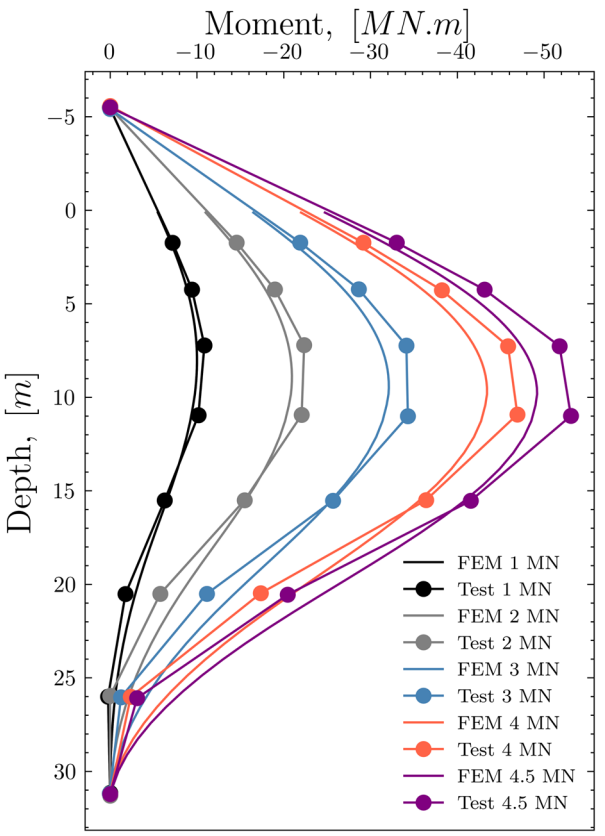

Figure 2. Bending moments for s/D of 0 under lateral loads of 1, 2, 3, 4 and 4.5 MN

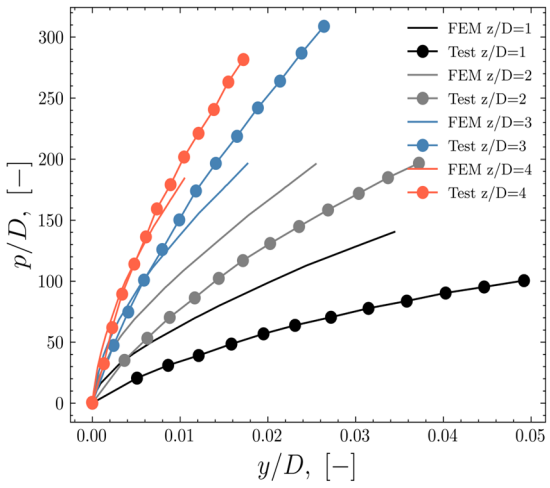

Figure 3. py curves for s/D of 0

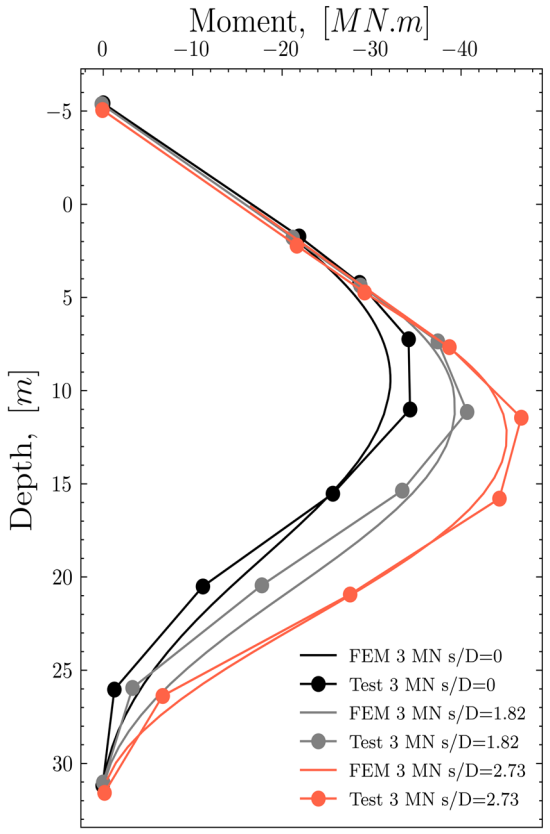

Figure 4. Bending moments for s/D of 0, 1.82 and 2.73, under a load of 3 MN

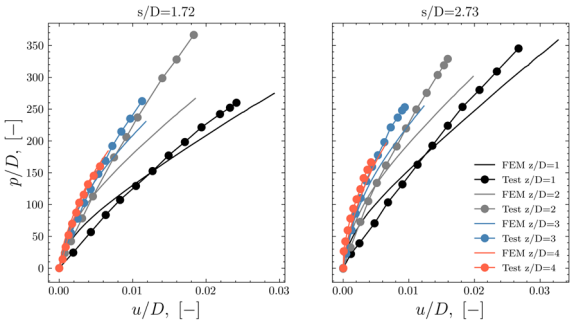

Figure 5. py curves at different depths for s/D of 1.72 and 2.73

4 NUMERICAL MODELING

This section will focus on the modeling of scour around a wind turbine monopile, using both 3D FEM and 1D beam column PISA models.

4.1 *Site conditions*

4.1.1 *Wind turbine*

The studied offshore wind turbine is located in the Belgian North Sea. The monopile is monitored using several devices such as Fibber Bragg Gratings (FBGs) for strain measurements along the monopile at selected depths. The OWT is supported by a monopile for which the geometrical characteristics are listed in the table below.

Table 2. Geometry of the studied monopile

h (m)	L (m)	t (mm)	D (m)
37	29.9	57-95	5

where h is the stick-up length, L is the monopile embedded length, t is the wall thickness and D is the monopile diameter.

4.1.2 *Soil*

The soil layering at the monopile location was established from boreholes and cone penetration tests (CPT) conducted at and around the monopile's location. The soil profile is shown in Figure 6. It consists of a 2 layered soil medium where the top 8 meters are represented by a medium-dense sand layer, while the lower part (up to 40 m below the seabed) is represented by an overconsolidated tertiary clay layer.

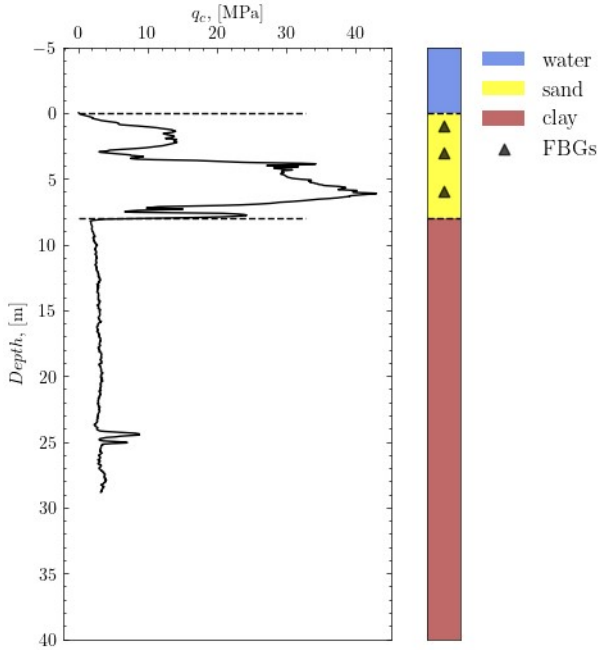

Figure 6. Cone resistance and soil layering at the wind turbine location

4.2 *Loads*

A set of quasi-static loading scenarios have been extracted from the monitoring data available on the studied wind turbine. The loads consist in a force and moment couple (F,M) that are applied directly on the monopile head. Every loading couple is paired with a monitored bending moment profile (generated by the loading couple). A total of 26 load cases have been derived for the studied monopiles, which are paired with 26 bending

moment profiles. More details on the methodology can be found in (Kheffache et al., 2024)

4.3 *Constitutive modeling*

Similar to the simulations carried out during the validation phase, the pile is modeled using an elastic model. Because of the difficulty associated with modeling a varying thickness of the monopile, a constant wall thickness has been assigned with a varying Young's modulus in order to keep a comparable bending stiffness EI between the in-situ monopile and the modeled one.

The soil is modeled using the hypoplastic clay and sand models (von Wolffersdorff, 1996; Mašín, 2013). These models have been previously calibrated for this specific wind turbine location using both advanced laboratory test and in-situ test data (Kheffache et al., 2024). Overall, the hypoplastic models give good control over the soil strength and stiffness, and more importantly, they can model the stiffness dependency on effective stress.

4.4 *Scour modeling and initial conditions*

The previously validated 3D FEM model is used to investigate the effect of soil scour on a monitored OWT under operational conditions. The resulting mesh on the 3D FEM model is shown in Figure 7. The both the soil and the pile were modeled using C3D8I elements, which are linear brick elements with incompatible modes, and are reputed to be better suited for the simulation of flexural behavior (bending) than the C3D8 elements.

The initial conditions that consist of an initial stress and void ratio profile are assigned to an unscoured soil model. The void ratio profile was established using water content measurements on a borehole located near the monopile's location. The stress was established using an earth pressure at rest coefficient K_0, which was calculated using the overconsolidation ratio (OCR) and the critical friction angle of the soil φ_c. In a second step, the soil volume corresponding to the scour is removed, and stress reduction is observed. Finally, a new analysis is performed where the initial conditions are specified at the last stress state achieved by the former analysis. The soil is first subjected to normalized scour depths s/D of 0, 1 and 1.4, which correspond to scour depths of 0, 5 and 7 m. The selected s/D values are well within the observed and recommended values for scour modeling (Mayall, 2019).

Moreover, a 1D beam column model that uses non-linear PISA reaction curves is also used to simulate the same problem. The scoured soil volume is just removed from the 1D model.

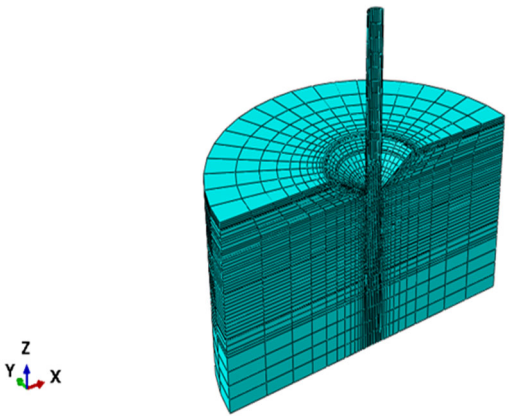

Figure 7. 3D FEM ABAQUS model of the pile and soil. Scour hole corresponding to s/D of 1.4

4.5 *Interface modeling*

The tangential monopile-soil interface is modeled in ABAQUS using a Mohr-Coulomb friction coefficient of 0.5. A "hard contact" behavior was assigned in the normal direction.

5 RESULTS AND DISCUSSIONS

The 3D FEM and 1D PISA models are subjected to the 26 load cases extracted from monitoring data, only one load case is show in Figure 8, for different s/D values for the sake of brevity. It can be seen that for s/D of 0, the 3D FEM predicts lower bending moments compared to 1D PISA, and closer values to the monitored bending moment profile, (monitoring values are also for s/D of 0, as the wind turbine did not suffer from any scour). This result has been widely discussed and reported before (Kheffache et al., 2024; 2025), and is due to the fact that in-situ monopiles are laterally stiffer than in both numerical models, and the 3D FEM models are able to replicate the stiffness better than the 1D PISA. It can be seen that an increase of s/D from 0 to 0.5, 1 and 1.4 leads to the increase of bending moment and the lowering of the point of maximum moment, under the same load, both in the 3D FEM and 1D PISA models. The point of maximal moment and its location are shown in Figure 9. It can be shown that under the same load, 3D FEM leads to lower maximum bending moment, and the point of application is higher when compared to the 1D PISA model

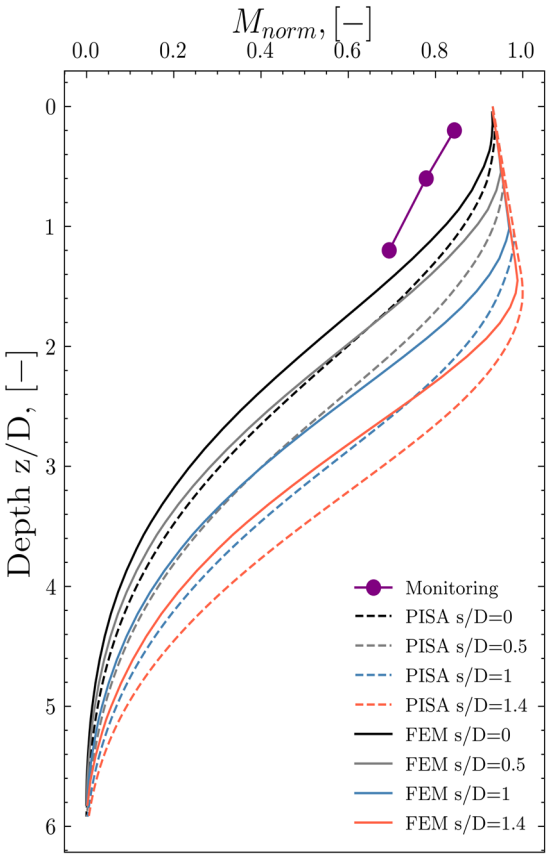

Figure 8. Normalized bending moments for different s/D values

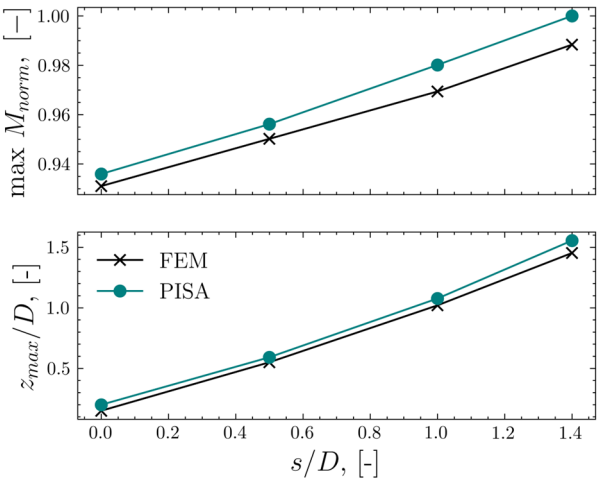

Figure 9. Maximum and location of the maximum bending moment as a function of s/D

The mismatch between the monitored and simulated bending moments are expressed in terms of the mean relative error (MRE), which is expressed according to the following equation:

$$MRE_M = \frac{1}{n}\sum_{i=0}^{n-1}\frac{M_m^{z,i} - M_s^{z,i}}{M_m^{z,i}}$$

where $M_m^{z,i}$ and $M_s^{z,i}$ are the monitored and simulated moments at sensor depth z for the i-th load case, and n is the total number of load case (26 in this work). Negative and positive values of MRE translate into an overestimation and underestimation of the simulated bending moments compared to the monitored ones respectively. The MRE values are shown in Figure 10. It can be seen that at each normalized sensor depth, an increase of s/D leads to an increase of MRE (in absolute value). The increase is however less pronounced at shallow levels compared to the deeper sensors, this can be due to the fact that an increase in s/D leads to the formation of a linear bending moment distribution (due to the loss of lateral support) at shallow depths. The MRE values issued from the 3D FEM model also seem to be lower than those from the 1D PISA model.

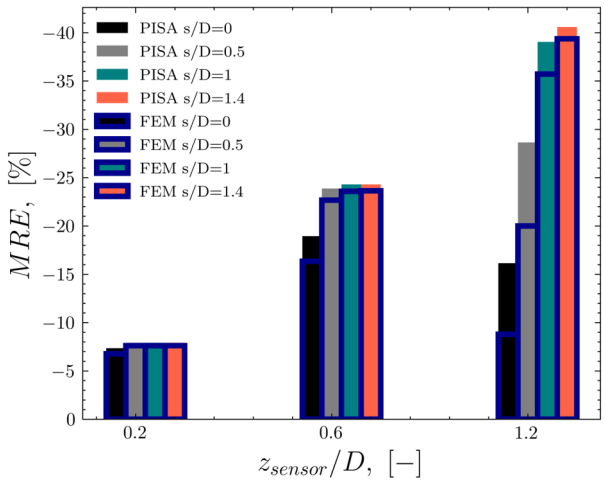

Figure 10. MRE at different sensor depths for different s/D values

The the GMRE, which is the mean of the MRE values is computed for both 3D FEM and 1D PISA, as it allows for a better visualization of the mismatch. It can be seen from Figure 11 that an increase of s/D from 0 to 1.4 leads to an increase of GMRE (in absolute value), translating an increase in bending moment mismatch with the monitoring data, which is caused by a loss of lateral stiffness and capacity. The GMRE values from 3D FEM are always lower than the 1D PISA ones, however the latter model is able to replicate the same trend of GMRE evolution with s/D compared to 3D FEM.

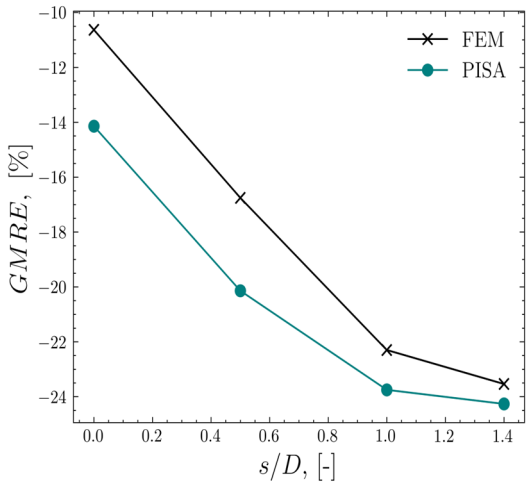

Figure 11. effect of s/D on the GMRE

6 CONCLUSIONS, RECOMMENDATIONS AND FUTURE WORK

This paper focuses on scour effects on an offshore wind turbine under operational conditions. A 3D FEM model was first developed and thoroughly validated using centrifuge tests from the literature. Different methods of scour simulation were also investigated, more precisely using a 1D method, which uses the PISA reaction curves. The following conclusions are made:

- Scour affects OWTs even under operational conditions, as it leads to the loss of lateral stiffness and capacity, which leads to increased bending moments under the same load conditions.
- The 1D PISA approach gave worse results (higher bending moments) than the 3D FEM one, however, the trends are comparable.
- A better methodology would be to extract the reaction curves from the 3D FEM and used them in the 1D PISA model.

This work highlighted the superiority of the 3D FEM approach when compared to the 1D rule-based PISA for modeling scour effects. Nonetheless, the 1D method was able to replicate the observed trends. Future works will focus on the comparison between scour protection stiffening effects using 3D FEM and the 1D PISA models.

ACKNOWLEDGEMENTS

The authors would like to acknowledge the support of the Belgian Ministry of Economic Affairs through the EFT project WINDSOIL project. The Support of VLAIO through the De Blauwe Cluster SBO SOILTWIN project is also acknowledged.

REFERENCES

Bienen, B., Fan, S., Schröder, M. and Randolph, M.F., 2021. Effect of the installation process on monopile lateral response. Proceedings of the Institution of Civil Engineers - Geotechnical Engineering, 174(5), pp.530–548. https://doi.org/10.1680/jgeen.20.00219.

Burd, H.J., Taborda, D.M.G., Zdravković, L., Abadie, C.N., Byrne, B.W., Houlsby, G.T., Gavin, K.G., Igoe, D.J.P., Jardine, R.J., Martin, C.M., McAdam, R.A., Pedro, A.M.G. and Potts, D.M., 2020. PISA design model for monopiles for offshore wind turbines: application to a marine sand. Géotechnique, 70(11), pp.1048–1066. https://doi.org/10.1680/jgeot.18.P.277.

Byrne, B.W., Houlsby, G.T., Burd, H.J., Gavin, K.G., Igoe, D.J.P., Jardine, R.J., Martin, C.M., McAdam, R.A., Potts, D.M., Taborda, D.M.G. and Zdravković, L., 2020. PISA design model for monopiles for offshore wind turbines: application to a stiff glacial clay till. Géotechnique, 70(11), pp.1030–1047. https://doi.org/10.1680/jgeot.18.P.255.

Deltares, 2023. Handbook of Scour and Cable Protection Methods. JIP HASPRO, Handbook Scour and Cable Protections.

Kallehave, D., Byrne, B.W., LeBlanc Thilsted, C. and Mikkelsen, K.K., 2015. Optimization of monopiles for offshore wind turbines. Philosophical Transactions of the Royal Society A: Mathematical, Physical and Engineering Sciences, 373(2035), p.20140100. https://doi.org/10.1098/rsta.2014.0100.

Kheffache, A., Stuyts, B., Jurado, C.S. and Devriendt, C., 2025. Bending moment profiles as indicators for the lateral stiff-ness of offshore wind turbines. [online] Available at: <https://www.issmge.org/uploads/publications/132/133/ISFOG2025-589.pdf> [Accessed 14 August 2025].

Kheffache, A., Stuyts, B., Sastre Jurado, C., Weijtjens, W., Devriendt, C. and Troch, P., 2024. Advanced simulations of monitored wind turbine monopiles located in the Belgian North Sea under operational quasi-static loading. Ocean Engineering, 311, p.118914. https://doi.org/10.1016/j.oceaneng.2024.118914.

Mašín, D., 2013. Clay hypoplasticity with explicitly defined asymptotic states. Acta Geotechnica, 8(5), pp.481–496. https://doi.org/10.1007/s11440-012-0199-y.

Mayall, R., 2019. Monopile response to scour and scour protection. [PhD Thesis] University of Oxford. Available at: <https://ora.ox.ac.uk/objects/uuid:2886ac08-c59e-409d-8d60-6724443d8d1a> [Accessed 14 August 2025].

Qi, W.G., Gao, F.P., Randolph, M.F. and Lehane, B.M., 2016. Scour effects on p–y curves for shallowly embedded piles in sand. Géotechnique, 66(8), pp.648–660. https://doi.org/10.1680/jgeot.15.P.157.

Spyridis, M. and Lopez-Querol, S., 2024. Installation of open-ended piles: A numerical investigation into the effects on the state of silica sand. Soils and Foundations, 64(3), p.101458.

Sumer, B.M. and Fredsøe, J., 2002. Time scale of scour around a large vertical cylinder in waves. In: ISOPE International Ocean and Polar Engineering Conference. [online] ISOPE. p.ISOPE-I. Available at: <https://onepetro.org/ISOPEIOPEC/proceedings-abstract/ISOPE02/All-ISOPE02/8763> [Accessed 14 August 2025].

von Wolffersdorff, P.-A., 1996. A hypoplastic relation for granular materials with a predefined limit state surface. Mechanics of Cohesive-frictional Materials, 1(3), pp.251–271. https://doi.org/10.1002/(SICI)1099-1484(199607)1:3<251::AID-CFM13>3.0.CO;2-3.